Journal of Catalysis **211,** 192–197 (2002)
doi:10.1006/jcat.2002.3717

Investigation of Reaction Steps for the Hydrodechlorination of Chlorine-Containing Organic Compounds on Pd Catalysts

Nan Chen, Robert M. Rioux, and Fabio H. Ribeiro[1]

Worcester Polytechnic Institute, Department of Chemical Engineering, Worcester, Massachusetts 01609-2280

Received March 11, 2002; revised June 6, 2002; accepted June 13, 2002

Reaction steps for the reaction of hydrodechlorination on Pd were investigated by means of isotope-exchange experiments. The reversibility of bond scission for the two C–Cl bonds in CF_3CFCl_2 was investigated by following ^{37}Cl enrichment in the reactant and products. No enrichment of ^{37}Cl was observed in the reactant CF_3CFCl_2 but the product CF_3CHFCl was enriched. Thus, the scission of the first C–Cl bond is irreversible; once the reactant loses the first chlorine it desorbs only as a product. However, after the first C–Cl bond is broken, the second chlorine may be exchanged with the pool of surface chlorine. Isotope exchange experiments between D_2 and HCl during hydrodechlorination of CF_3CFCl_2 showed that the forward rate and reverse rate for the overall reaction $H_2 + 2Cl* = 2HCl + 2*$ were nearly 400 times faster than the overall hydrodechlorination reaction rate. Thus, this experiment confirms that this step is in quasi-equilibrium. © 2002 Elsevier Science (USA)

Key Words: **hydrodechlorination on Pd: reaction steps; hydrodechlorination on Pd: isotope exchange.**

INTRODUCTION

Hydrodechlorination is the reaction between H_2 and an organic molecule containing a C–Cl bond to form HCl and a C–H bond. Hydrodechlorination is an important step in many syntheses that use a chlorine-containing molecule as an intermediate. For example, hydrodechlorination is used in the manufacture of CF_3CFH_2 (a widely used refrigerant) from CF_3CFCl_2 (1) and in the manufacture of $CHCl_3$ or CH_2Cl_2 from CCl_4 (2). Another recent application of dechlorination in the presence of H_2 is in the conversion of a byproduct into a useful compound, for example, in the conversion of 1,2-dichloropropane into propylene (3) on a bimetallic Pt–Cu catalyst.

Turnover rates, selectivity, and reaction orders have been presented for a limited number of compounds (4–11). Some studies have dealt with possible reaction steps, similar to the ones presented in this work (7, 8, 12–17). Ribeiro *et al.* (7) and Thompson *et al.* (4) suggested that the rate-determining step might be the scission of the carbon–chlorine bond, possibly as an oxidative addition forming a Pd–Cl and a Pd–C bond on the same catalytic site; that chlorine is the most abundant reaction intermediate; and that HCl and H_2 are in equilibrium with adsorbed H and Cl. An updated version of the mechanism follows. The first step is the equilibrated adsorption of the reactant with an equilibrium constant K_{CFC}:

$$CF_3CFCl_2 + * = CF_3CFCl_2 * . \qquad [1]$$

This step is followed by the scission of the first C–Cl bond, which is the rate-determining step with rate constant k_0:

$$CF_3CFCl_2 * \rightarrow \cdots . \qquad [2]$$

Note that the reaction products formed after this step are not kinetically significant and thus do not need to be represented. Steps [1] and [2] lead to the following rate expression:

$$r = k_0 K_{CFC}[CF_3CFCl_2][*] \qquad [3]$$

To calculate the number of empty sites ([*]) we assume the following equilibrium for H_2 and HCl with the surface:

$$H_2 + 2* = 2H* \qquad [4]$$

$$H* + Cl* = HCl + 2* \qquad [5]$$

The overall reaction that includes reactions [4] and (two times) [5] with equilibrium constant K_0 is

$$H_2 + 2Cl* = 2HCl + 2* \qquad [6]$$

Assuming that Cl* is the most abundant surface intermediate ($[*] + [Cl*] = [L]$) leads to the following expression for free-site concentration:

$$[*] = \frac{[L]}{1 + \frac{[HCl]}{K_0^{1/2}[H_2]^{1/2}}}. \qquad [7]$$

Finally, by substituting Eq. [7] into Eq. [3] with $k =$

---

[1] To whom correspondence should be addressed. E-mail: fabio@wpi.edu.

0021-9517/02 $35.00

$k_0 K_{CFC}[L]$ and $K = K_0^{-1/2}$, the rate is calculated as

$$r = \frac{k[CF_3CFCl_2]}{1 + K\frac{[HCl]}{[H_2]^{1/2}}}. \qquad [8]$$

These reaction steps were deduced from kinetic measurements only. Another very powerful technique to study reaction steps is isotope exchange, which is the objective of this contribution. Only a limited number of isotope-exchange studies have been conducted on the hydrodechlorination reaction. Campbell and Kemball (18) found that the reaction of C_2H_5Cl with D_2 on Pd films seemed to proceed through a carbene-like intermediate since the product ethane was significantly enriched with the doubly deuterated product CH_3CHD_2. As described in the following, chlorofluorocarbons (CFCs) seem to show unique behavior during isotope exchange. One example is the reaction of CF_3CFHCl with deuterium on Pd/C. The most abundant product was the monodeuterated product CF_3CFHD instead of the double-deuterated product as found in Campbell and Kemball's experiment. Chlorine exchange using $H^{37}Cl$ was also performed to show the irreversibility of the C–Cl bond cleavage, Eq. [2], which is assumed to be the rate-determining step in the proposed reaction mechanism. Step [6] was shown to be in quasi-equilibrium by measurements using deuterium exchange.

EXPERIMENTAL METHODS

Catalysts

Two palladium catalysts supported on carbon were used in this study. The 5% Pd catalyst supported on an activated carbon (5% Pd/C) was obtained from Degussa. The second carbon-supported catalyst (0.5% Pd/C) was prepared in-house via an incipient wetness procedure on an activated carbon manufactured by the Cabot Corporation (Sterling Series). The incipient wetness method utilized an aqueous solution of $PdCl_2$ (Aldrich, 99.99%) with the addition of 2 mol of HCl per mole of precursor with additional heating to aid the dissolution of $PdCl_2$. More information on the carbon-supported catalyst can be found in a previous publication (4). The supported samples were ground with a mortar and pestle and 40/60 mesh particles were retained for use in catalytic studies.

Reactant

The CFC 114a (CF_3CFCl_2) sample was obtained from DuPont, and HCFC 124 (CF_3CFHCl) from DuPont Suva Refrigerants. Mixtures of 15–20% HCl in He were purchased from Matheson and were made with technical-grade HCl and Matheson purity He. Hydrogen gas (Matheson) contained 1033 ppm of CH_4, which was used as an internal standard for the calibration of the gas chromatograph. Before it was fed into the reactor system, the hydrogen-methane mixture was passed through a packed bed containing a 5% Pd/C catalyst to eliminate any oxygen from the H_2 mixture. The hydrogen gas used for catalyst reduction was purified with a Pd membrane hydrogen purifier (Matheson hydrogen purifier model 8361). The deuterium was obtained from Cambridge Isotope Laboratories. It contained 99.6% D_2 and 0.4% HD, and before use it was passed through the same Pd membrane purifier used for purification of H_2. The $H^{37}Cl$ gas was purchased from Icon Services, Inc., and the $H^{37}Cl$ concentration was higher than 99%.

Reactor Configuration

The gas manifold was constructed of $\frac{1}{8}$-in.-diameter stainless steel tubing. Gas flow was controlled with mass flow controllers (Porter Instrument Co.). The reaction portion of the flow system was made of Pyrex glass. The reactor was made out of quartz with the catalyst held on a fritted disk. Reaction rates were measured in a well-mixed reactor operated in batch or continuous stirred tank reactor (CSTR) mode. Temperature was measured through a thermocouple well extended into the catalyst bed. The mixing in the CSTR was provided by a bellows pump (Senior Flexonics, MB-21) with a rate of about 1400 $cm^3\ min^{-1}$ allowing differential operation for the reactor and minimizing heat and transport effects in the reaction. Inlet and effluent flow rates were around 100 $cm^3\ min^{-1}$.

The reaction gases were injected with a gas valve or syringe into a modified GC-MS (GC-HP 5880A, MS-HP5970A). The column used in the GC was a 5% Krytox 143AC, 60/80 Carbopack B HT 20 ft × $\frac{1}{8}$ in. from Supelco. The effluent from the GC column was simultaneously analyzed by the GC flame ionization detector (for quantitative analysis) and by the MS (for qualitative analysis). The gas was sampled into the MS through a fused silica polyimide capillary (i.d. 51 μm, o.d. 363 μm) of 0.75-m length. The GC response factor for all reactants and products was calibrated against methane in a hydrogen–methane calibrated mixture. After exiting the system, the gases flowed through an NaOH solution to neutralize the HCl present in the effluent stream.

Data Collection Procedure

Two to five hundred milligrams of fresh catalyst was initially loaded into the reactor and reduced for 3 h at 300°C with 50 $cm^3\ min^{-1}$ H_2. For repeated experiments, the catalyst was treated with 50 $cm^3\ min^{-1}$ H_2 for 0.5–1 h at 150°C before the hydrodechlorination reaction.

The reactor was evacuated to 1×10^{-5} Torr for 0.5 hour before the gas reactants were fed into it. The oven temperature was raised to the target temperature at a rate of 5°C min^{-1}. The gas mixture was taken from the reactor using a 500-μl syringe through a GC septum fitted to a union mounted on the sample port of the batch reactor. For each data point, 100–200 μl of the gas mixture was injected into the GC-MS for analysis.

When the reactor was operated in CSTR mode, the inlet-gas concentrations were adjusted with mass flow controllers. For a particular set of conditions, 30 to 60 min were allotted for the reaction to reach steady state, at which time the first data point was taken. The gas mixture was sampled into the GC-MS system using an automatic valve on the GC-MS. To ensure that deactivation had not occurred during the duration of the experiment, the reaction conditions for the first point in the series were repeated at the end of each experiment.

Surface Area Measurement

The total surface area was measured using the BET method with N_2. The Pd metal surface area was measured by the hydrogen–oxygen titration method according to Benson *et al.* (19). The experimental setup consisted of a volumetric system constructed in Pyrex and pumped by a liquid nitrogen trapped diffusion pump. The amount of gas adsorbed was determined by measuring pressure change in a precalibrated volume on the system with a pressure transducer (MKS model 127).

The samples were reduced in flowing H_2 (50 cm^3 min^{-1}) for 3 h at 300°C before the Pd surface area measurements were carried out. After the initial reduction, subsequent hydrogen–oxygen titrations were conducted at 100°C. The crystallite size, based on chemisorption measurements, was estimated from the expression d (nm) = 112/(percentage of metal exposed [PME]). This expression is valid for spherical particles and a Pd atom density of 1.27×10^{19} atoms m^{-2} (20).

X-ray diffraction (Rigaku Geigerflex diffractometer) of reduced and passivated catalysts was also conducted. Samples for XRD analysis were reduced in the same manner as described earlier and then passivated with 60 Torr of O_2. Particle size was determined from the width of the diffraction peak using the X-ray line-broadening technique. The Scherrer equation was used to calculate Pd particle size with appropriate correction for instrumental line broadening.

Error Analysis

We compared the data for the same experiment carried out at identical conditions to calculate experimental errors. Turnover rate reproducibility was better than 90%.

RESULTS AND DISCUSSION

Catalyst Properties

Table 1 summarizes the properties of the catalysts employed. Non-microporous carbon supports were used in all experiments. Based on the results of previous research, it was found that CFC reactants may condense in the pores of microporous carbon, leading to a lower reaction order in CFC (4).

TABLE 1

Catalyst Properties

Catalyst	BET surface area (m^2 g^{-1})	Amount of surface Pd (μmol g^{-1})	PME[a] (%)	Particle diameter (nm) Chemisorption[b]	Particle diameter (nm) XRD
0.5% Pd/C	29	3.8	8.0	14	14
5.0% Pd/C	107	39.1	8.4	13	5

[a] Percentage of metal exposed, determined by H_2–O_2 titration at 100°C.
[b] Particle size determined from d = 112/PME.

Particle size determined by XRD line broadening is also shown in Table 1. There is good agreement between chemisorption and XRD particle sizes for the 0.5% Pd/C sample. On the other hand, the Pd particle size measured by XRD for the 5.0% Pd/C catalyst is about three times smaller than that determined by chemisorption, which suggests that the particles are formed by a number of smaller agglomerates.

The parameters in Table 1 are representative of catalysts before reaction. Since no significant deactivation was observed during reaction, no significant change in the properties of the catalyst is expected after reaction.

The presence of heat and mass transfer limitations was tested using the Madon–Boudart test (21, 22). From the results presented in previous work (4), no heat and mass transfer limitations were found, even with the highest-surface-area catalyst, where transport limitations would be most severe. Thus, we concluded that these artifacts did not affect the results.

Determination of reversibility of C–Cl bond scission in CF_3CFCl_2. In a previous publication (4), a correlation between the C–Cl bond energy and the rate of hydrodechlorination for a series of CFCs was observed, suggesting that the scission of the first C–Cl in the CFC is irreversible and rate-determining. The objective of this section is to investigate whether the C–Cl-bond-breaking process is reversible. We employed CF_3CFCl_2 for this purpose since its kinetics have been studied in detail (4, 7, 8, 23). As indicated in Scheme 1, two C–Cl bonds are involved. As explained next,

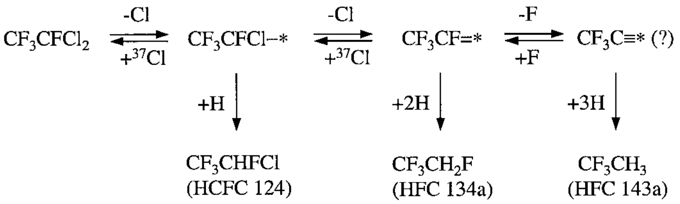

SCHEME 1. Proposed reaction network for the CF_3CFCl_2 hydrodechlorination reaction on a surface saturated with ^{37}Cl.

the reversibility of the steps can be investigated using ^{37}Cl isotope-exchange methods.

To investigate the reversibility of the various steps, the surface was saturated with ^{37}Cl from H^{37}Cl. When a C–Cl bond in the probe molecule is broken and subsequently reformed, the molecule shows enrichment in chlorine if the chlorine from the molecule can exchange with adsorbed ^{37}Cl on the surface. The ^{37}Cl saturation on the surface can be achieved because HCl adsorbs on the surface preferentially, making Cl the most abundant reaction intermediate. Also, as shown below, the rate of exchange of adsorbed chlorine with gas-phase HCl (Eq. [6]) is 400 times faster than the hydrodechlorination rate. Thus, a high pressure of H^{37}Cl in the initial mixture ensured a surface saturated with ^{37}Cl.

For CF_3CFCl_2 there are two chlorine atoms that can undergo hydrodechlorination or isotope exchange. Scheme 1 shows the reactions that might happen on the surface pretreated with H^{37}Cl. To monitor the scission of C–Cl bonds, the chlorine isotope distributions on the reactant CF_3CFCl_2 and on the product CF_3CHFCl (HCFC124) are analyzed. The data for the hydrodechlorination experiment using CF_3CFCl_2 with H^{37}Cl were collected at three different CF_3CFCl_2 pressures (230, 136, and 52 Torr), 80 Torr of H^{37}Cl, and a balance of H_2 (480, 574, and 658 Torr) for a total pressure of 790 Torr. Blank experiments with unlabeled HCl were also performed under the same conditions. The turnover rate and selectivity of the experiments with H^{37}Cl were comparable to the results from unlabeled HCl experiments. A total of 36 data points with H^{37}Cl were collected with conversion levels as high as 20%. The chlorine isotope distribution in CF_3CFCl_2 was calculated using the ion at m/e 135 (and 137), which is the most intense and corresponds to the monochlorinated species CF_3CFCl. Because only one chlorine is present, the ratio of intensities at m/e 135 to the one at 137 give the isotope distribution of chlorine in CF_3CFCl_2 directly. The ratio of the total amount of ^{35}Cl to ^{37}Cl in CF_3CFCl_2 was found to be in the range 2.99 ± 0.07, close to the natural abundance of 3.1. As an additional check, we report the relative intensities of the fragment CCl_2F at m/e 105, 103, and 101, which gives the distribution of chlorine corresponding to the three compounds $CF_3CF^{37}Cl^{37}Cl : CF_3CF^{35}Cl^{37}Cl : CF_3CF^{35}Cl^{35}Cl$, and should occur naturally in the ratio 0.058 : 0.365 : 0.578. The average distribution for the H^{37}Cl experiments is 0.062, 0.361, and 0.577 and for unlabeled HCl is 0.063, 0.363, and 0.575 with a standard deviation of 0.003 for each distribution point. Since no enrichment in the reactant was observed, it was suggested that the rate of exchange was lower than our analytical detection limit. The minimum reverse reaction rate that would cause a detectable deviation in the ^{35}Cl-to-^{37}Cl ratio was calculated to be 5.1×10^{-4} s^{-1}, while the turnover rate of the hydrodechlorination reaction at the same condition was 5–6 $\times 10^{-2}$ s^{-1}, which can be taken as the forward C–Cl bond scission reaction rate. Upon comparison of these two rates, we can conclude that the first C–Cl bond scission is irreversible.

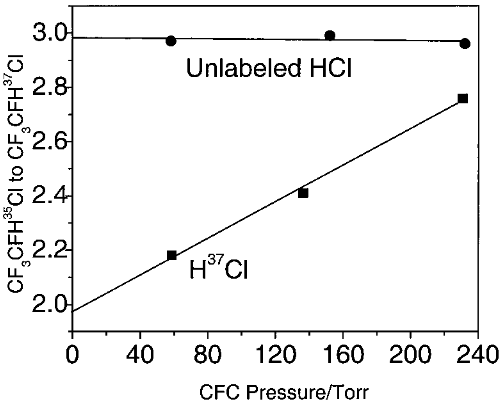

FIG. 1. Enrichment of CF_3CFHCl in ^{37}Cl as a result of the reversibility of chlorination steps on the surface. Hydrodechlorination reaction of CF_3CFCl_2 carried out at the specified pressure, 480 Torr H_2, 80 Torr H^{37}Cl, and 150°C in a batch reactor. Selectivity was independent of conversion.

The ratio $CF_3CHF^{35}Cl : CF_3CHF^{37}Cl$ for the product CF_3CHFCl was monitored to determine the reversibility of breaking the second C–Cl bond. This ratio was found to be independent of conversion, less than the natural ratio of 3.1, and dependent on initial reactant partial pressure (Fig. 1). Blank experiments with unlabeled HCl were conducted under the same CF_3CFCl_2 partial pressures as used in the H^{37}Cl experiments to verify that no artifacts were responsible for the decrease in the $CF_3CHF^{35}Cl : CF_3CHF^{37}Cl$ ratio. In all blank experiments, the $CF_3CHF^{35}Cl : CF_3CHF^{37}Cl$ ratio was close to 3.1, the natural ratio (Fig. 1). The blank and isotope experiments confirm that switching the reactant from unlabeled HCl to H^{37}Cl alone causes the ratio $CF_3CHF^{35}Cl : CF_3CHF^{37}Cl$ to change. Thus, it is concluded that for some of the C–Cl bonds the exchange reaction is reversible.

Explanations of why the ratio $CF_3CHF^{35}Cl : CF_3CHF^{37}Cl$ is a function of CF_3CFCl_2 and H_2 partial pressure and why the exchange ratio at zero pressure of CF_3CFCl_2 (infinite dilution) approaches 2.0 could not be quantitatively explained. As shown in Scheme 1, this is a multistep reaction network with a complex dependence of rates on partial pressures. It is easy to understand, however, that even at infinite dilution of CF_3CFCl_2 on the surface the exchange ratio will not be zero because the $CF_3CFCl{-}*$ intermediate can be hydrogenated without ever exchanging chlorine. The possibility that ^{35}Cl from the reaction dilutes ^{37}Cl on the surface and thus decreases the exchange ratio in Fig. 1 does not seem feasible. As shown next, the rate of exchange of surface chlorine with gas-phase H^{37}Cl is much faster than the hydrodechlorination reaction.

Measurement of the forward and reverse rate for the reaction between gas-phase H_2 and HCl and adsorbed H and Cl atoms. In the proposed CFC hydrodechlorination reaction steps shown in Eqs. [4]–[6], it is assumed that H_2 and HCl are in equilibrium with the corresponding adsorbed atomic species on the surface, and that the rate-determining step is the scission of carbon–chlorine bond in the CFC molecule. If this is true, the magnitude of the rate forward or reverse for reaction [6] should be much larger than the overall rate of reaction, and the difference between the two rates equal to the overall turnover rate. To measure the forward and reverse rates, isotope exchange was used.

Deuterium was substituted for hydrogen to measure the rate of the forward and reverse reaction in Eq. [6]. In the experiment, a mixture of 436-Torr D_2, 65.5-Torr unlabled HCl, 209-Torr CF_3CFCl_2, and 19.2-Torr Ar (a mass spectrometer internal standard) were fed into a batch reactor preheated to reaction temperature (150°C).

It can be seen that because D_2 was used, Cl will react on the surface through Eq. [5] to produce DCl instead of HCl. This can easily be distinguished from the initial HCl fed into the system with a mass spectrometer. Thus, the rate of the forward reaction can be related to formation of DCl, while the reverse-reaction rate can be related to the disappearance of HCl. The ion abundance of $H^{37}Cl$ and $D^{37}Cl$ were monitored as a function of time with a mass spectrometer and then related to their respective partial pressures to quantify the forward- and reverse-reaction rates. In Fig. 2, the variation of $H^{37}Cl$ and $D^{37}Cl$ signal was plotted as a function of time. Note that time zero as defined in Fig. 2 is arbitrary and does not correspond to the start of reaction; data was collected before the gas stream was directed into the reactor.

Figure 2 shows that the exchange reaction was equilibrated in less than 60 s. From the volume of the batch reactor (0.1347 L), the DCl formation rate was 7.5 s^{-1} and the rate of $H^{37}Cl$ consumption rate was 6.4 s^{-1}. Thus the overall rate is four times higher than the rate of $H^{37}Cl$ consumption, since the other 76% of the mixture is $H^{35}Cl$, or about 30 s^{-1}. The CF_3CFCl_2 hydrodechlorination rate measured in the same experiment was 7.4×10^{-2} s^{-1}. From these rates, we conclude that the C–Cl bond scission process is about 400 times slower than the reaction between gas-phase H_2, HCl, and surface H, Cl atoms.

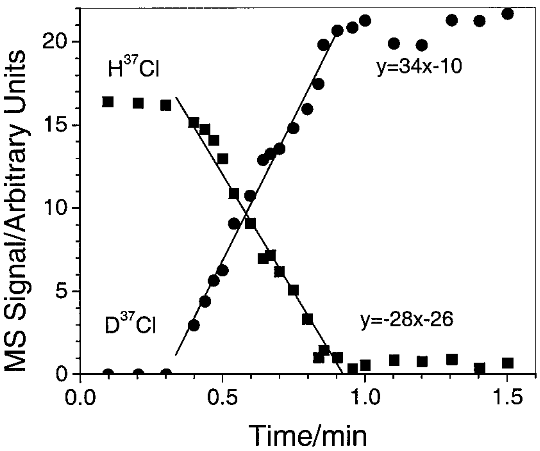

FIG. 2. Variation of $H^{37}Cl$ and $D^{37}Cl$ pressure with time during hydrodechlorination of CF_3CFCl_2 (209 Torr) at 150°C with 436-Torr D_2, 65.5-Torr HCl, and 19.2-Torr Ar in a batch reactor.

Note that for DCl and HCl in Fig. 2 the MS signal was not adjusted for the relative sensitivities. Due to the primary isotope effect, HCl molecules are more easily fragmented than DCl molecules when ionized in the mass spectrometer. The result is that for the same amount of $D^{37}Cl$ and $H^{37}Cl$, the ion intensity of unfragmented $D^{37}Cl$ (mass 39) is higher than that for $H^{37}Cl$ (mass 38) (24). In Fig. 2, this is the reason for a higher signal of DCl at the end than the initial signal of HCl and also a higher absolute value of the slope for DCl. To calculate the forward and reverse rates we are also assuming that other reactions involving these species are negligible. In conclusion, the magnitude of the forward or reverse rate is about 400 times higher than the rate of hydrodechlorination. Thus, the assumption that Eq. [6] is quasi-equilibrated is supported by these results.

Investigation of reaction steps beyond the rate-determining step and possible surface intermediates. The proposed reaction steps in Eqs. [1]–[8] succeeded in predicting the overall kinetics, but it cannot explain the observed product distribution. Prediction of product selectivity can only be achieved by understanding the reaction steps beyond the rate-determining step.

Deuterium substitution was used to study the hydrodechlorination of HCFC124 (CF_3CFHCl) as reported before for Pd black (23). The experiment was conducted in a batch reactor, enabling a wide conversion range (16–54%) at one temperature. The selectivity of all products was found to be independent of conversion. In the CF_3CHFCl molecule, the carbon containing the chlorine atom also contains a hydrogen atom. Calculations with Gaussian 98 software (25) indicated that in the gas phase the C–H bond strength is almost 100 kJ mol^{-1} higher than the C–Cl bond. Considering only the bond strength as a variable, it is expected that the C–H bonds should not break at the conditions under which the C–Cl bond breaks. In fact, the product distribution contains 98.3% CF_3CFHD and only 1.5% CF_3CFD_2. From the isotope distribution it is believed that $CF_3CFH{-}*$ should be present on the Pd surface. For the case of CF_3CFCl_2, it can be concluded from the product distribution that $CF_3CFCl{-}*$ and $CF_3CF{=}*$ species are formed on the surface (Scheme 1). It is surprising, however, that although the C–F on the chlorine carbon is also almost 100 kJ mol^{-1} stronger than the C–Cl bond, it is broken about 5% of the time. These examples illustrate the difficulty in predicting the product distribution for this reaction.

SUMMARY

Isotope exchange experiments were employed to verify the reaction steps of CFC hydrodechlorination reactions. It was found that the scission of the first C–Cl bond in CF_3CFCl_2 is irreversible, while the scission of the second C–Cl bond is reversible. Thus, once the reactant adsorbs and the first C–Cl bond is broken, it can exchange other chlorine atoms but the molecule desorbs only as a product. Deuterium exchange experiments with HCl showed that adsorbed H and Cl are in equilibrium with gas-phase H_2 and HCl, with the rate forward or reverse for the step $H_2 + 2Cl{*} = 2HCl + 2{*}$ almost 400 times higher than the overall hydrodechlorination reaction rate. The deuterium-labeling experiment with CF_3CFHCl showed that most of the time only the C–Cl bond breaks. It is deduced that $CF_3CFH{*}$ is the major surface species. The explanation of selectivity still remains a challenge; a more complete reaction sequence beyond the rate-determining step must be assembled before selectivity can be estimated.

ACKNOWLEDGMENTS

We gratefully thank the National Science Foundation for funding through grant CTS-9702699. We thank Degussa for the 5% Pd/C catalyst and DuPont for a sample of CF_3CFCl_2.

REFERENCES

1. Ainbinder, Z., Manzer, L. E., and Nappa, M., *in* "Handbook of Heterogeneous Catalysis" (J. Weitkamp, Ed.), Vol. 4, p. 1677. VCH, Weinheim, 1997.
2. Mullin, C. R., and Wymore, C. E., The Dow Chemical Company, U.S. Patent No. 3,579,596 (1971).
3. Harley, A. D., Holbrook, M. T., Smith, D. D., Cisneros, M. D., Ito, L. N., and Murchison, C. B., The Dow Chemical Company, U.S. Patent No. 5,453,557 (1995).
4. Thompson, C. D., Rioux, R. M., Chen, N., and Ribeiro, F. H., *J. Phys. Chem. B* **104**, 3067 (2000).
5. Early, K., Kovalchuk, V. I., Lonyi, F., Desmukh, S., and d'Itri, J., *J. Catal.* **182**, 219 (1999).
6. Karpinski, Z., Early, K., and d'Itri, J., *J. Catal.* **164**, 378 (1996).
7. Ribeiro, F. H., Gerken, C. A., Somorjai, G. A., Kellner, C. S., Coulston, G. W., Manzer, L. E., and Abrams, L., *Catal. Lett.* **45**, 149 (1997).
8. Ribeiro, F. H., Gerken, C. A., Rupprechter, G., Somorjai, G. A., Kellner, C. S., Coulston, G. W., Manzer, L. E., and Abrams, L., *J. Catal.* **176**, 352 (1998).
9. Rupprechter, G., and Somorjai, G. A., *Catal. Lett.* **48**, 17 (1997).
10. Coq, B., Figuéras, F., Hub, S., and Tournigant, D., *J. Phys. Chem.* **99**, 11159 (1995).
11. Ribeiro, F. H., and Somorjai, G. A., *Am. Chem. Soc. Symp. Ser.* **766**, 192 (2001).
12. Bodnariuk, P., Coq, B., Ferrat, G., and Figueras, F., *J. Catal.* **116**, 459 (1989).
13. Coq, B., Ferrat, G., and Figueras, F., *J. Catal.* **101**, 434 (1986).
14. Deshmukh, S., and d'Itri, J. L., *Catal. Today* **40**, 377 (1998).
15. van de Sandt, E. J. A. X., Wiersma, A., Makkee, M., van Bekkum, H., and Moulijn, J. A., *Recl. Trav. Chim. Pays-Bas* **115**, 505 (1996).
16. Buelow, M. T., Immaraporn, B., and Gellman, A. J., *J. Catal.* **203**, 41 (2001).
17. Buelow, M. T., and Gellman, A. J., *J. Am. Chem. Soc.* **123**, 1440 (2001).
18. Campbell, J. S., and Kemball, C., *Trans. Faraday Soc.* **57**, 809 (1961).
19. Benson, J. E., Hwang, H. S., and Boudart, M., *J. Catal.* **30**, 146 (1973).
20. Anderson, J. R., *in* "Structure of Metallic Catalysts," p. 296. Academic Press, New York, 1975.
21. Koros, R. M., and Nowak, E. J., *Chem. Eng. Sci.* **22**, 470 (1962).
22. Madon, R. J., and Boudart, M., *Ind. Eng. Chem. Fundam.* **21**, 438 (1982).
23. Rioux, R. M., Chen, N., and Ribeiro, F. H., *Catal. Today* **62**, 269 (2000).
24. Millard, B. J., *in* "Quantitative Mass Spectroscopy," p. 67. Heyden, London, 1978.
25. Foresman, J. B., and Frish, A., "Exploring Chemistry with Electronic Structure Methods." 2nd ed., Gaussian, Pittsburgh, 1996.